ACS OMEGA

http://pubs.acs.org/journal/acsodf

Article

Study on Occluding Dentinal Tubules with a Nanosilver-Loaded Silica System In Vitro

Yang Zhou, Meng Yang, Qingjie Jia, Guojun Miao, Leilei Wan, and Yi Zhang*

Cite This: *ACS Omega* 2021, 6, 19596−19605

Read Online

ACCESS | Metrics & More | Article Recommendations | Supporting Information

ABSTRACT: The effects of most clinical treatments for dentin hypersensitivity are not long-lasting. To overcome the defects, the mesoporous silica nanoparticles and silver nanoparticles entered the field of oral materials. This study aimed to synthesize a novel, low-cytotoxic dentin desensitizer and investigate its occlusion effects on dentinal tubules. The biphasic stratification approach, a chemical reduction method, and the Stöber method were used to synthesize silver nanoparticle-loaded and nonporous silica-encapsulated mesoporous silica (Ag-MSNs@nSiO$_2$), which was a noncrystalline structure with an average size of approximately 128 nm and a silver content of 3.506%. Atomic absorption spectrometry and the 3-(4,5-dimethylthiazol-2-yl)-2, 5-diphenyltetrazolium bromide cell viability assay showed that Ag-MSNs@nSiO$_2$ slowly released silver ions and had nearly no cytotoxicity. An electron microscope was used to observe the blocking effects on the dentinal tubules of sensitive tooth disc models, which were randomly divided into the following four groups: a deionized water group, a 5.9 M silver nitrate solution group, an Ag-MSNs@nSiO$_2$ group, and a Gluma desensitizer group. There were no significant differences in the relative area of open dentinal tubules between the Ag-MSNs@nSiO$_2$ group and the Gluma desensitizer group ($P > 0.05$). Detection of protein structures showed that multilevel structures of bovine serum albumin in dentin tubules were significantly changed by silver ions from Ag-MSNs@nSiO$_2$. These results suggest that nearly noncytotoxic Ag-MSNs@nSiO$_2$ was successfully synthesized by a series of methods. Ag-MSNs@nSiO$_2$ occluded dentin tubules immediately and effectively. Moreover, the blockage effects may be enhanced and maintained by continuous condensation of proteins in dentinal tubules.

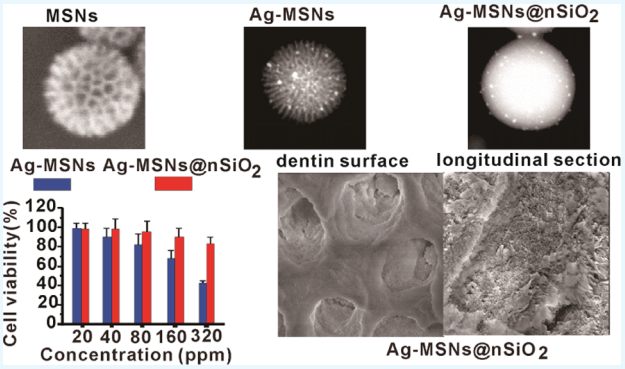

INTRODUCTION

Dentin hypersensitivity is a common disease in dental clinics characterized by transient and sharp pain caused by temperature and mechanical or chemical stimulation.[1] It is hypothesized that external stimuli cause fluid flow in the dentin tubules, stimulating sensory nerve endings and causing dentin hypersensitivity.[2] Therefore, the current clinical methods for the treatment of dentin hypersensitivity are to seal dentinal tubules, such as nerve desensitization, protein precipitation, dentinal tubule plugging, and dentin adhesive sealing.[3] However, the effects of most dentin desensitizers are not long-lasting because the blocked dentinal tubules on the dentin surface are usually re-exposed in response to dietary abrasion.[4] Therefore, a new desensitizer is needed to block dentin tubules effectively and lastingly.

Mesoporous silica nanoparticles (MSN) has many good properties, for example, a unique hollow structure, a large surface area/mass ratio, a high stability, low cytotoxicity, and so on. It has been widely used in the biomedical field and often used as the ideal mediator for medicines and genes.[5] Recent studies showed that MSNs could resist dietary acid and mechanically fill dentin tubules to treat dentin hypersensitivity.[6] Some substances were loaded to MSNs to increase the efficacies. For example, Tian et al. found that MSNs had both desensitization and antibacterial effects on dentin with incorporated epigallocatechin-3-gallate, Ca^{2+}, and P.[7] Because silver ions denatured and coagulated proteins and had extensive antibacterial effects, the addition of silver was the most common method for synthesizing biomedical materials.[8,9] Silver nanoparticles (AgNPs), a new material, have a significant increase in antibacterial effects compared with silver.[10] However, high concentrations of silver ions resulted in blackened teeth and corroded mucous membranes, affecting the aesthetics of teeth and damaging tissues.[11] AgNPs can also be changed significantly in terms of physical and chemical

Received: April 21, 2021
Accepted: July 12, 2021
Published: July 20, 2021

properties and toxicity,[12] which makes it possible the return of silver to the field of oral materials.

Some studies have reported the effects of AgNP-loaded MSNs (Ag-MSNs) on blocking the dentinal tubules. For example, Jung et al. reported that a silver-doped bioactive glass/mesoporous silica nanocomposite successfully blocked the dentinal tubules, in which silver ions and bioactive glasses were added to increase bioactivity.[13] In addition to mechanically blocking dentinal tubules, silver ions slowly released from Ag-MSNs could continuously coagulate proteins to block dentinal tubules, which has not been reported. Moreover, there were no reports on reduction in the cytotoxicity of Ag-MSNs. To control the release of silver ions and their cytotoxicity, coating Ag-MSN with a shell is worthy of study.

This study is designed to synthesize a novel, low-cytotoxic dentin desensitizer, AgNP-loaded and nonporous silica-encapsulated mesoporous silica (Ag-MSNs@nSiO_2), and to investigate its cytotoxicity, mechanically blocking effects on dentin tubules and the effects on protein aggregation in dentin tubules.

MATERIALS AND METHODS

This study was conducted in accordance with the standards outlined in the American Chemical Society's Ethical Guidelines to Publication of Chemical Research and was approved by the Medical Ethics Committee of Chenggong Hospital, Fujian Medical College, China (approval number 2017XJS-001-01). Oral and written informed consents had been obtained from all donors. No unexpected or unusually high safety hazards were encountered.

Chemicals and Reagents. Cyclohexane, ammonium nitrate, silver nitrate, cetyltrimethyl ammonium chloride (CTAC), sodium citrate, sodium borohydride, ammonia water, and anhydrous ethanol were purchased from Sinopharm Chemical Reagent Company Limited, Shanghai, China. Triethanolamine and anhydrous toluene were bought from Xilong Scientific Company Limited, Shantou, Guangdong, China. Tetraethyl orthosilicate was obtained from Alfa Aesar Chemical Reagent Company Limited, Shanghai, China. 3-Aminopropyltrimethoxysilane was acquired from Aladdin Industrial Corporation, Shanghai, China. Bovine serum albumin (BSA) and 3-(4,5-dimethylthiazol-2-yl)-2,5-diphenyl-tetrazolium bromide (MTT) were purchased from Sigma-Aldrich, Saint Louis, Missouri, USA.

Synthesis of Ag-MSNs@nSiO_2. First of all, the mesoporous silica nanoparticles were achieved via the biphase stratification approach as reported with a little modification.[14] 48 mL of (25 wt %) CTAC solution and 0.36 g of TEA were added to 72 mL of water and stirred gently at 60 °C for 1 h in a 250 mL round-bottomed flask. Then, 40 mL of (20 v/v %) TEOS in cyclohexane was carefully added to the water−CTAC−TEA solution, and the mixture was kept at 60 °C in an oil bath under magnetic stirring. The reaction system was maintained at 60 °C for 24 h. MSNs were obtained after being extracted with a 0.6 wt % ammonium nitrate (NH_4NO_3) ethanol solution at 60 °C for 18 h. The amino-functional MSNs (amino-MSNs) were achieved via a postgrafting strategy. 10 mL of toluene, 50 mg of MSNs, and 1 mL of 3-aminopropyltriethoxysilane were mixed and stirred in a constant temperature oil bath at 110 °C for 8 h. The amino-MSNs were lyophilized to obtain the dry powder after being washed several times with ethanol. Nanosilver-decorated MSNs (Ag-MSNs) were synthesized through a chemical reduction method.[15] 10 mL 5.6 mg/mL amino-MSN water dispersion and 6 mL 0.425 mg/mL silver nitrate aqueous solution were mixed. Then, 0.1 mg/mL sodium citrate aqueous solution and 0.01 M sodium borohydride aqueous solution were added to synthesize Ag-MSNs. Finally, the Stöber method[16] was used to coat the shell of Ag-MSNs. 1 mL of 10 mg/mL Ag-MSNs water dispersion was mixed with 8 mL ethanol and 80 μL of ammonia water. 60 or 120 μL of TEOS was added to the mixture above to obtain products named as Ag-MSNs@nSiO_2-60 and Ag-MSNs@nSiO_2-120. The products were lyophilized, stored at 4° C, and protected from light until the next use.

Testing of the Material Characteristics. Scanning electron microscopy (SEM; SUPRA 55 SAPPHIRE; Zeiss, Baden-Wurttemberg, Germany) and transmission electron microscopy (TEM; Tecnai F30, Philips-FEI, Amsterdam, Netherlands) were used to obtain the morphology of the samples. The morphology of the MSNs was observed using SUPRA 55 SAPPHIRE at 10 kV. The size distribution of Ag-MSNs@nSiO_2 was obtained by calculating the size of nanoparticles in the micrograph at a magnification of $10^5\times$. TEM, high-angle annular dark field imaging in the scanning TEM (HAADF−STEM), and energy-dispersive spectroscopy (EDS) observations were performed on a Tecnai F30 transmission electron microscope with an accelerating voltage of 200 kV equipped with a postcolumn Gatan imaging filter (GIF-Tridium). For TEM measurements, the samples were dispersed in ethanol and then dried on a holey carbon film Cu grid.

Inductively coupled plasma atomic emission spectroscopy (ICP-AES; IRIS Intrepid II XSP; Thermo Fisher Scientific incorporated, Waltham, Massachusetts, USA) was used to measure the silver content of Ag-MSNs@nSiO_2. An X-ray powder diffraction (XRD) investigation was carried out with a polycrystal X-ray diffractometer (Rigaku Corporation, Tokyo, Japan) using Cu Kα radiation. Fourier transform infrared (FTIR) spectra were recorded with a spectrophotometer (Nicolet iS50 FT-IR; Thermo Fisher Scientific incorporated, Waltham, Massachusetts, USA) using KBr pellets. Nitrogen adsorption−desorption measurements were conducted with a porosity analyzer (ASAP 2020M; Micromeritics Instrument Corporation, Atlanta, Georgia, USA). The Brunauer−Emmett−Teller (BET) specific surface area (ABET) was calculated from the adsorption data in the relative pressure (P/P_0) ranging from 0.04 to 0.1. The pore size (D_p) distribution was calculated from the adsorption branch of the isotherms using the Barrett−Joyner−Halenda (BJH) formula.

Release of Silver Ions In Vitro. To test the releasing rate of silver ions, we used atomic absorption spectrometry (AAS; Shimadzu, Tokyo, Japan). The dispersions of Ag-MSNs@nSiO_2 and Ag-MSNs at the same concentration were prepared using simulated body fluid (SBF) as the solvent. After being protected from light in a 37 °C water bath, the supernatants were collected at the time points of 0.5, 1, 2, 4, 12, 24, 48, 72, 96, and 120 h. The concentration of silver ions was measured by AAS. Then, the actual concentration of silver ions at every time point was calculated according to the following formula[17]

$$C_{tcorr} = C_t + \frac{\nu}{V}\sum_{0}^{t-1} C_t$$

https://doi.org/10.1021/acsomega.1c02123
ACS Omega 2021, 6, 19596−19605

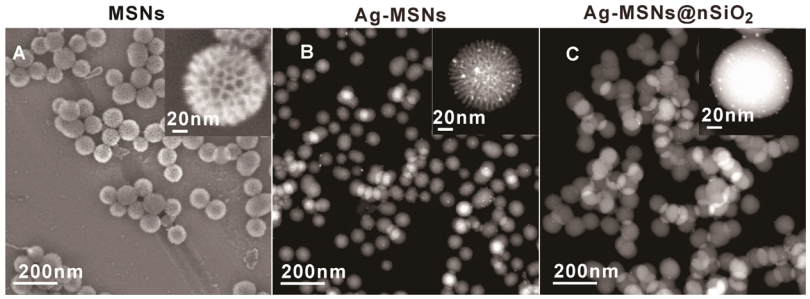

Figure 1. Morphology. SEM images of MSNs (A), TEM images of Ag-MSNs (B), and TEM images of Ag-MSNs@nSiO$_2$ (C). Abbreviations:mesoporous silica nanoparticles (MSNs), silver nanoparticle-loaded MSNs (Ag-MSNs), and silver nanoparticle-loaded and nonporous silica-encapsulated mesoporous silica (Ag-MSNs@nSiO$_2$).

C_{tcorr} is the actual concentration of silver ions released at time t, C_t is the concentration of silver ions in the sample removed at time t, ν is the volume of the release medium removed and V is the total volume of the release medium.

The SBF contained the following (g/L):[18] NaCl, 7.996; $NaHCO_3$, 0.350; KCl, 0.224; $K_2HPO_4{\cdot}3H_2O$, 0.228; $MgCl_2{\cdot}6H_2O$, 0.305; $CaCl_2$, 0.278; and $Na2_SO_4$, 0.071, adjusted to pH 7.35 with Tris.

For comparison, the experiment was repeated three times.

Cytotoxicity Assessment. Cytotoxicity assays are among the first in vitro bioassay methods used to predict toxicity of substances.[19] Mouse embryonic fibroblasts (NIH-3T3; China Center for Type Culture Collection, Wuhan, Hubei, China) were cultivated in α-modified essential medium (Dulbecco's modified Eagle's medium; LM001-01; Welgene Company, Seoul, South Korea) supplemented with 10% (v/v) fetal bovine serum, penicillin (100 U/mL), and streptomycin (100 μg/mL) at 37 °C under 5% CO_2.

The cytotoxicity of Ag-MSNs@nSiO$_2$ against NIH-3T3 was examined using the MTT cell viability assay. First, NIH-3T3 with a cell density of 5*10^4/mL was planted on a 96-well plate at a volume of 200 μL/well. Subsequently, a series of concentrations of MSNs, Ag-MSNs, and Ag-MSNs@nSiO$_2$ were added to the wells so that final concentrations became 0, 10, 20, 40, 80, 160, and 320 μg/μL, and incubated for 24, 72, and 120 h. Then, MTT (5 mg/mL) was added to the wells and incubated for another 2 h at 37 °C. The optical density (OD) value at 490 nm wavelength was measured using an enzyme-labeled instrument (POLARstar Omega; BMG Labtech, Offenburg, Germany). The cell viability of the blank control (untreated cells) was set as "100%" and the absorbance of each sample was compared to that of the blank control. For comparison, the experiment was repeated three times.

Specimen Preparation and Experimental Design of Dentinal Tubular Occlusion. Premolars of humans free of defects and caries, which were extracted as part of orthodontic treatment, were obtained after informed consent had been given and stored in 0.5% thymol solution at 4 °C. Using a low-speed diamond saw (SYJ-160; Milliren Technologies incorporated, Northern California, USA), a 1 mm-thick dentin disc was obtained 1 mm above the enamel. The central area of the dentin disc with a diameter of 5 mm was defined as the experimental area, polished with a 600-mesh, a 800-mesh, and 1000-mesh grit silicon carbide (Hubei Yuli sand belt Company Limited, Wuhan, China) for 30 s, pretreated with 6% citric acid (Ping an Medical Equipment Trading Company Limited, Hua county, Henan, China) for 20 s, cleaned with deionized water for 1 min, and kept in 0.5% thymol solution at 4 °C.

Before experimenting, the specimens were pretreated with 2% BSA (Cohn Fraction V, pH 5.2; SIGMA ALDRICH, Saint Louis, Missouri, USA) aspirated into the dentin tubules to simulate the components of fluid proteins in dentinal tubules.[20] Ag-MSNs@nSiO$_2$ powders were mixed with SBF to obtain 2, 4, and 6% Ag-MSNs@nSiO$_2$ dispersions. Then, a dentin disc was divided into four equal parts, three parts were treated with 2, 4, and 6% Ag-MSNs@nSiO$_2$ dispersions using the gas pressurization technique,[21] and then their occlusion effects were compared.

Twenty-five dentin disks were selected randomly. Each dentin disc was divided into four equal parts and then treated as described above with deionized water, 5.9 M silver nitrate ($AgNO_3$) solution, 4% Ag-MSNs@nSiO$_2$, and Gluma desensitizers (Heraeus Kutzer, Wehrheim, Germany) to observe the staining effects and tubule-occluding effects on the dentin surface. Then, each part was cut into half to observe the longitudinal section. All dentin specimens were desiccated, Au−Pd alloy sputter-coated, and observed using a scanning electron microscope at 5 kV.

The occluding degree on the dentinal surface was quantified using scanning electron microscopy and image analysis (Image-Pro PLUS 6.0; Media Cybernetics, Maryland, USA).[22] Three images were taken at a constant magnification of ×1000 with a 50 μm scale bar from the central portion of each sample. The images were saved as TIF files for image analysis and the relative area of open dentinal tubules was calculated.

The length of the precipitate in the dentinal tubules was measured from the dentinal surface to the bottom of the precipitate.

Detection of Multilevel Structural Changes of Bovine Serum Albumin in Silver Ion Solution. The powders were mixed with SBF to obtain 4% Ag-MSNs@nSiO$_2$ dispersions. After 24 or 120 h at 37 °C, the supernatants of the dispersions were obtained after filtration and centrifugation and named Ag^+ (24 h) and Ag^+ (120 h). The silver ion concentrations were detected by ICP−AES. The $AgNO_3$ solution was prepared with the same concentration as that of Ag^+ (24 h).

2% BSA was mixed with SBF, Ag^+ (24 h), Ag^+ (120 h), and $AgNO_3$ solution at 37 °C for 24 h. The secondary structures of BSA were detected by circular dichroism (CD) spectroscopy (J-810; JASCO Corporation, Tokyo, Japan), and the spectra were measured in a 1 cm path length cell with a measurement range of 190−260 nm at 0.5 nm intervals and a scan speed of 200 nm/min. CDSSTR software (available at http://lamar.colostate. edu/~sreeram/CDPro) was used to obtain the secondary structure content data.[23] Ultraviolet and visible

https://doi.org/10.1021/acsomega.1c02123
ACS Omega 2021, 6, 19596−19605

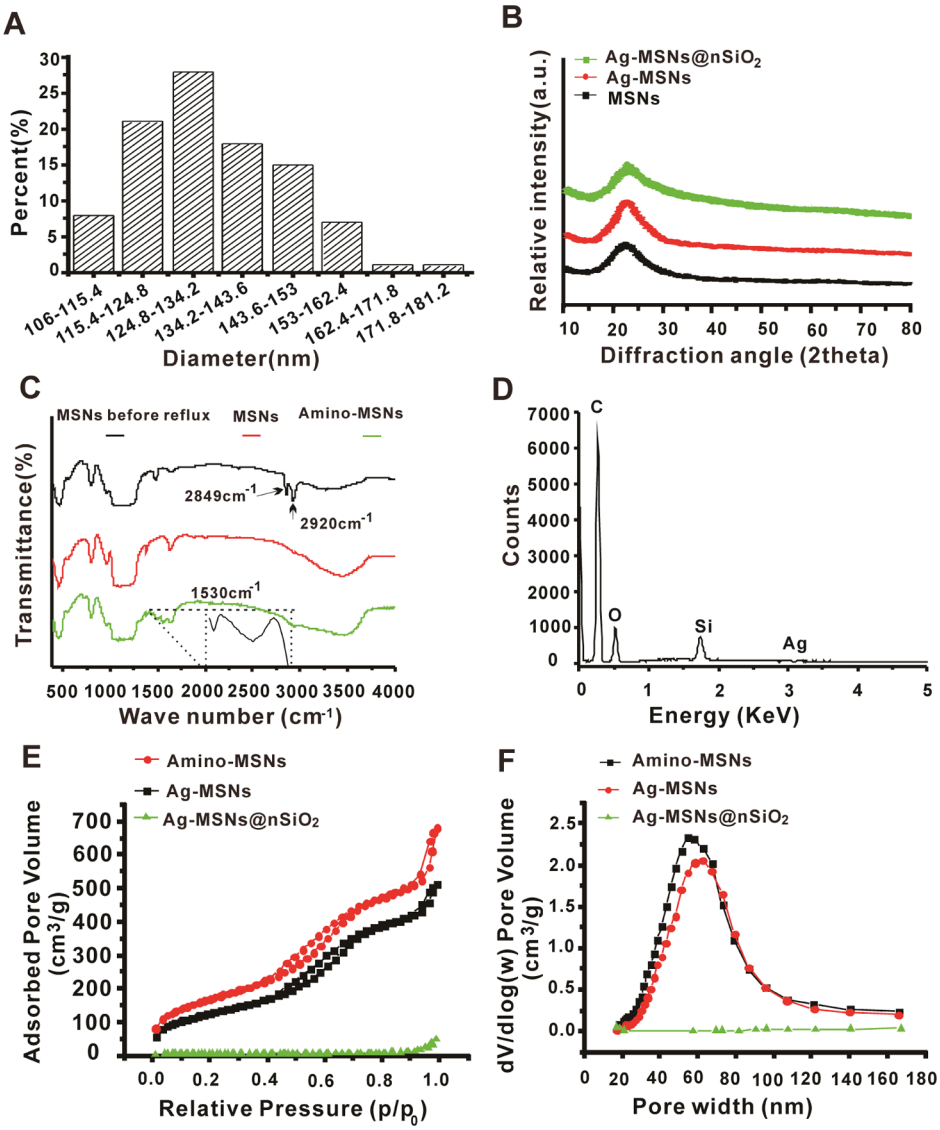

Figure 2. Characterization of materials. (A) Size distribution of Ag-MSNs@nSiO$_2$. (B) X-ray powder diffraction patterns of MSNs, Ag-MSNs, and Ag-MSNs@nSiO$_2$. (C) Fourier transform infrared spectra of semifinished MSNs, MSNs, and amino-MSNs. (D) EDS of Ag-MSNs. (E) Nitrogen adsorption−desorption isotherms. (F) Pore volume distribution of amino-MSNs, Ag-MSNs, and Ag-MSNs@nSiO$_2$. Abbreviations: mesoporous silica nanoparticles (MSNs), silver nanoparticle-loaded MSNs (Ag-MSNs), silver nanoparticle-loaded and nonporous silica-encapsulated mesoporous silica (Ag-MSNs@nSiO$_2$), and MSNs modified by the amino group (amino-MSNs).

spectroscopy (UV-2600; Unico instrument Company Limited, Shanghai, China) was employed to observe the conformational changes of BSA through scanning in the ultraviolet range of 190−350 nm with the $AgNO_3$ solution as a reference. Dynamic light scattering (DLS; MPT-2; Malvern Instruments Limited, Shanghai, China) was employed to detect the BSA molecular hydrodynamic radius (Rh) and the particle size distribution.

Statistical Analyses. The data were analyzed using Origin 7.5 software (OriginLab, Northampton, Massachusetts, USA) and were shown as mean ± SD. Student's t-test was applied to analyze the significant differences when evaluating the release rate of silver ions, the relative cell viability, the dentinal tubule-occluding effects, and the size distributions of BSA. $P < 0.05$ was considered statistically significant.

RESULTS

Morphology of the Materials. To observe the morphological change of the materials during the synthesis, SEM and TEM were employed. The SEM image confirmed that MSNs have a spherical porous structure (Figure 1A). The TEM image of Ag-MSNs at a high magnification showed that bright spots of silver nanoparticles were uniformly distributed in MSNs (Figure 1B). The TEM image of Ag-MSNs@nSiO$_2$ (Figure 1C) showed that a uniform silica layer was generated on the surface of Ag-MSNs with incorporated bright spots. These results suggest that Ag-MSNs@nSiO$_2$ was successfully synthesized.

Characterization. *Particle Size.* Figure 2A shows that the average size of Ag-MSNs@nSiO$_2$ was approximately 128 nm according to TEM.

X-Ray Diffraction. To study the material types, wide-angle X-ray powder diffraction was applied. The samples of MSNs, Ag-MSNs, and Ag-MSNs@nSiO$_2$ showed a noncrystalline structure between 10 and 35° (Figure 2B), implying that the material was amorphous.

https://doi.org/10.1021/acsomega.1c02123
ACS Omega 2021, 6, 19596−19605

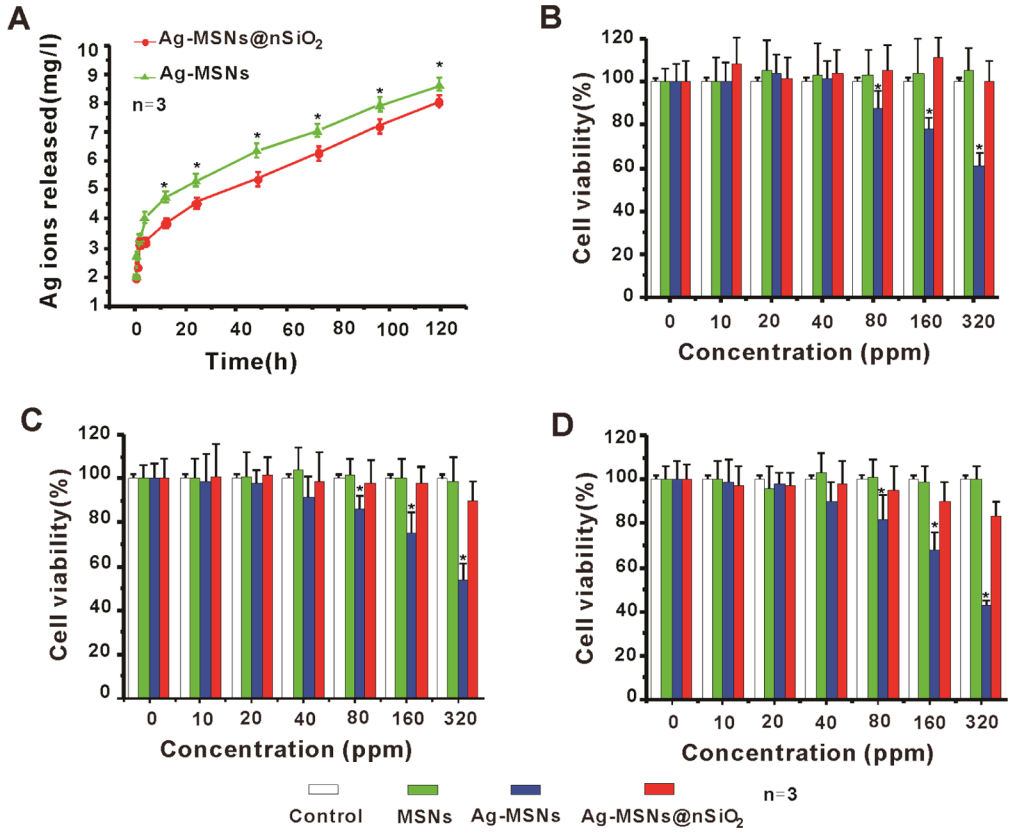

Figure 3. Release of silver ions and cytotoxicity of materials. (A) Release of silver ions from Ag-MSNs and Ag-MSNs@nSiO$_2$ (*P < 0.05 vs Ag-MSNs@nSiO$_2$; n = 3). (B−D) Relative cell viability of MSNs, Ag-MSNs, and Ag-MSNs@nSiO$_2$ at different concentrations (0−320 μg mL^{-1}) for 24 (B), 72 (C), and 120 h (D) (*P < 0.05 vs Ag-MSNs@nSiO$_2$; n = 3). Abbreviations: mesoporous silica nanoparticles (MSNs), silver nanoparticle-loaded MSNs (Ag-MSNs), and silver nanoparticle-loaded and nonporous silica-encapsulated mesoporous silica (Ag-MSNs@nSiO$_2$).

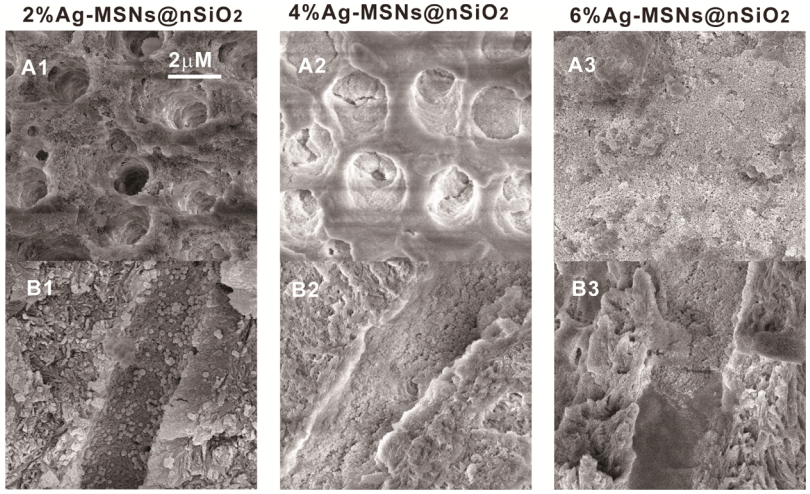

Figure 4. Tubule-occluding effects of 2, 4, and 6% Ag-MSNs@nSiO$_2$. SEM images of 2, 4, and 6% Ag-MSNs@nSiO$_2$ occluding dentin tubules on the dentin surface (A1−A3) and in the longitudinal section (B1−B3). Abbreviations: mesoporous silica nanoparticles (MSNs), silver nanoparticle-loaded MSNs (Ag-MSNs), silver nanoparticle-loaded, and nonporous silica-encapsulated mesoporous silica (Ag-MSNs@nSiO$_2$).

Fourier Transform Infrared Spectroscopy. To detect whether the cytotoxic intrapore surfactant, CTAC, was extracted during the synthesis process, Fourier transform infrared spectroscopy was performed. Figure 2C shows that the strong absorption bands at approximately 2849 and 2920 cm^{-1} disappeared after reflux, demonstrating that CTAC was successfully extracted. Additionally, an absorption band at 1530 cm^{-1} appeared after amino modification, implying that an amino group was present as a linking agent (amino-MSNs).

Detection of Silver in Ag-MSNs. EDS analysis of Ag-MSNs indicated an atomic Ag/Si ratio of 1:87 (Figure 2D), confirming the existence of silver nanoparticles. ICP-AES showed that the silver content in Ag-MSNs@nSiO$_2$ was 3.506%.

https://doi.org/10.1021/acsomega.1c02123
ACS Omega 2021, 6, 19596−19605

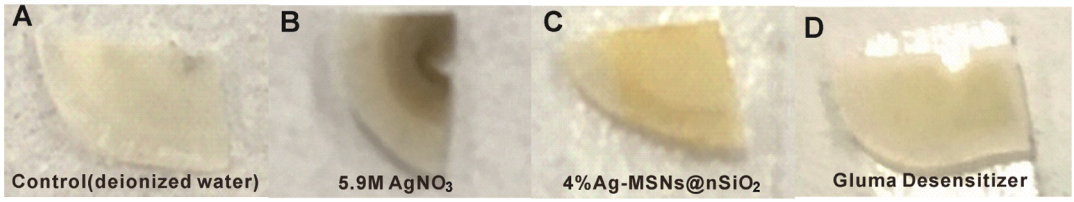

Figure 5. Effects of Ag-MSNs@nSiO$_2$ on dentin color. Effects of deionized water (A), 5.9 M AgNO$_3$ (B), 4% Ag-MSNs@nSiO$_2$ (C), and Gluma desensitizer (D) on the dentin color. Abbreviations: silver nanoparticle-loaded and nonporous silica-encapsulated mesoporous silica (Ag-MSNs@nSiO$_2$) and silver nitrate (AgNO$_3$).

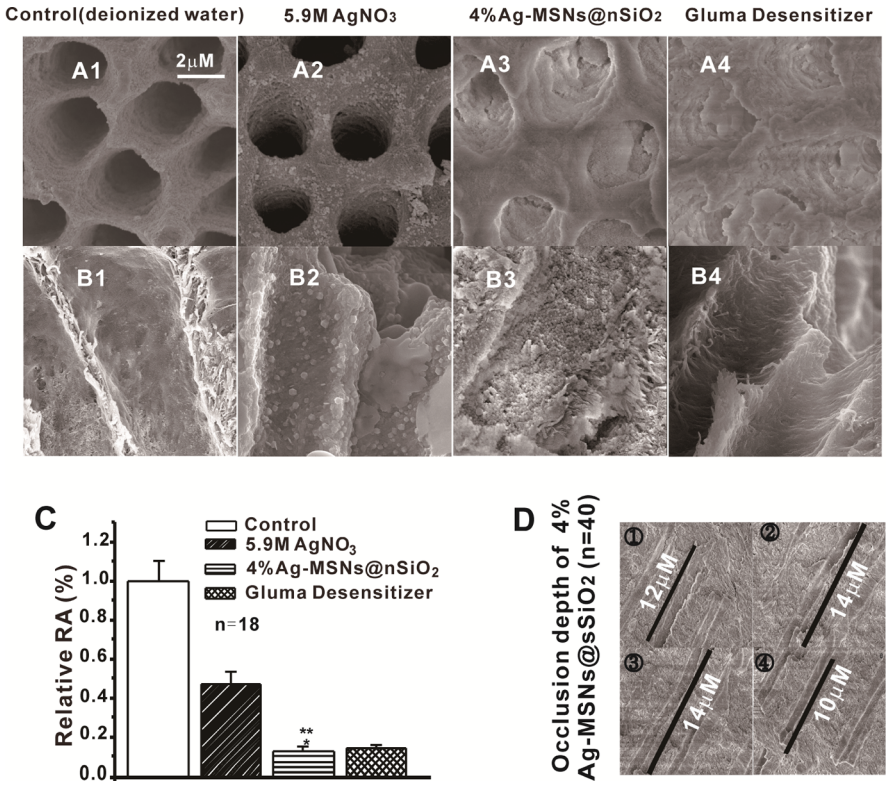

Figure 6. Tubule-occluding effects of Ag-MSNs@nSiO$_2$ on dentin. (A1−A4) SEM images on the dentin surface of deionized water, 5.9 M AgNO$_3$, Ag-MSNs@nSiO$_2$, and Gluma desensitizers occluding dentin tubules. (B1−B4) SEM images in longitudinal section of deionized water, 5.9 M AgNO$_3$, Ag-MSNs@nSiO$_2$, and Gluma desensitizers occluding dentin tubules. (C) Relative area of opened dentinal tubules (*P < 0.05 vs 5.9 M AgNO$_3$; **P > 0.05 vs Gluma desensitizer; n = 18). (D) Occlusion depth of 4% Ag-MSNs@nSiO$_2$. Abbreviations: silver nanoparticle-loaded and nonporous silica-encapsulated mesoporous silica (Ag-MSNs@nSiO$_2$) and silver nitrate (AgNO$_3$). The relative area of opened dentinal tubules (RA).

N_2 Adsorption. To assess the porosity of amino-MSNs, Ag-MSNs, and Ag-MSNs@nSiO$_2$, the nitrogen adsorption isotherm was measured and found to display a type IV isotherm, which was associated with the presence of mesopores, except for Ag-MSNs@nSiO$_2$. Before and after silver was loaded into amino-MSNs, the Brunauer−Emmett−Teller (BET) surface area (Figure 2E, red/black) decreased from 604.30 to 455.70 m^2/g, while the pore volume (Figure 2F, black/red) decreased from 0.86 to 0.70 cm^3/g and the pore diameters decreased from 5.20 to 5.10 nm. After nonporous silica coating, the BET surface area (Figure 2E, green) decreased to 19.50 m^2/g, and the pore volume and pore diameter were 0.01 cm^3/g and 1.30 nm (Figure 2F, green), respectively. The results indicated that AgNPs were loaded into the pores of MSNs and the SiO$_2$ film covered the entire sphere.

Release Profiles of Silver Ions. To study the influence of the nonporous silica shell on silver ion release, atomic absorption spectrometry was used to evaluate the release rate of silver ions. Figure 3A shows that silver ions rapidly released during the initial 12 h, then gradually increased until 120 h, with silver ion concentrations within 9 ppm. The concentrations of silver ions released from the Ag-MSNs@nSiO$_2$ were significantly lower than those from the Ag-MSNs at 12, 24, 48, 72, 96, and 120 h (*P < 0.05 vs Ag-MSNs@nSiO$_2$; n = 3), indicating that the SiO$_2$ coating significantly reduced the release of silver ions.

Cytotoxicity Assay. Figure 3B−D shows that the relative cell viability of Ag-MSNs@nSiO$_2$ groups were almost 100%, except 90% in 72 h groups at a concentration of 320 μg mL^{-1}, and 91, 83% in 120 h groups at a concentration of 160, 320 μg mL^{-1}. While the relative cell viability of Ag-MSN groups decreased significantly at high concentrations (80, 160, and 320 μg mL^{-1}), 88, 78, 61% in 24 h groups, and 85, 74, 54% in 72 h groups, and 81, 67, 43% in 120 h groups, respectively.

Effects of Ag-MSNs@nSiO$_2$ on Dentin. *Tubule-Occluding Effects of 2, 4, and 6% Ag-MSNs@nSiO$_2$.* To find the

https://doi.org/10.1021/acsomega.1c02123
ACS Omega 2021, 6, 19596−19605

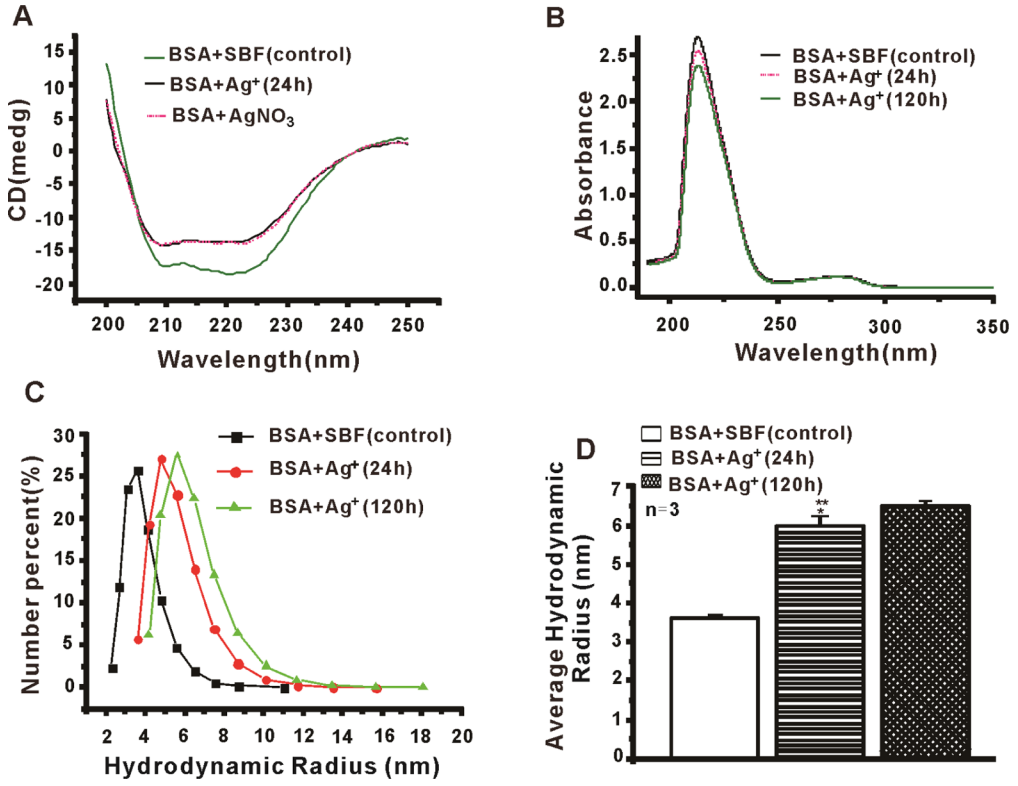

Figure 7. Effects of silver ions on BSA. (A) CD spectra. (B) UV−vis absorption spectra. (C) Size distributions of molecular hydrodynamic radius. (D) Comparison of the average molecular hydrodynamic radius in BSA + SBF, BSA + Ag^+ (24 h), and BSA + Ag^+ (120 h) (*P < 0.05 vs control; **P > 0.05 vs BSA + Ag^+ (120 h); n = 3). Abbreviations: bovine serum albumin (BSA), simulated body fluid (SBF), the supernatants of 4% Ag-MSNs@$n$$SiO_2$ dispersions mixed for 24 h [Ag^+ (24 h)], silver nitrate solution with the same concentration as that of Ag^+ (24 h) ($AgNO_3$), the supernatants of 4% Ag-MSNs@$n$$SiO_2$ dispersions mixed for 120 h [Ag^+ (120 h)].

appropriate plugging concentration of Ag-MSNS@$n$$SiO_2$, 2, 4, and 6% dispersions were selected for comparative experiments. On the dentin surface (Figure 4A1−A3), the higher the concentration, the better the occluding effects; however, in the longitudinal section (Figure 4B1−B3), the occluding depth of the 4% group was significantly higher than that of the 6% group, which was only approximately 3 μm from the mouth of the dentin tubules, indicating that the best occluding concentration was 4%.

Effects of Ag-MSNs@$n$$SiO_2$ on Dentin Color. To study the effects of 4% Ag-MSNs@$n$$SiO_2$ on the dentin color, we compared the staining effects of four different desensitizers on dentins. 5.9 M $AgNO_3$ solution blackened the teeth (Figure 5B), and a similar color was observed for the Gluma group and the control group (Figure 5A,D), while the 4% Ag-MSNs@$n$$SiO_2$ resulted in a light yellow dentin color (Figure 5C).

Comparison of Tubule-Occluding Effects of Deionized Water, 5.9 M $AgNO_3$, 4% Ag-MSNs@$nSiO_2$, and Gluma Desensitizers. To study the dentinal tubule-occluding effects of 4% Ag-MSNs@$n$$SiO_2$, tubule-occluding effects of four different desensitizers were compared using SEM. Deionized water could not occlude the dentinal tubules (Figure 6A1,B1); the 5.9 M $AgNO_3$ group (Figure 6A2,B2) showed many particles adhered to the inner wall of the tubules but no particles on the surface; both 4% Ag-MSNs@$n$$SiO_2$ and the Gluma desensitizer almost completely occluded the dentinal tubules on the dentin surface (Figure 6A3,A4). The Ag-MSNs@$n$$SiO_2$ precipitates adhered to the tubular inner wall (Figure 6B3) at a penetration depth of 50.78 ± 0.30 μm (Figure 6D, n = 40). The Gluma precipitates on the tubular inner wall were similar to diaphragms (Figure 6B4).

The relative area of open dentinal tubules was calculated to quantify the occluding degree on the dentinal surface. The relative area of the control was 0.18 ± 0.10. The relative area of Ag-MSNs@$n$$SiO_2$ decreased from 100% for the control to 12.69 ± 1.16%, which was significantly lower than that of 5.9 M $AgNO_3$ (from 100% for the control to 47.21 ± 6.03%), but no significant difference from that of the Gluma desensitizer (from 100% for the control to 14.49 ± 1.368%) (Figure 6C; *P < 0.05 vs 5.9 M $AgNO_3$; **P > 0.05 vs Gluma desensitizer; n = 18). The results suggested that the tubule-occluding effects of Ag-MSNs@$n$$SiO_2$ on the dentin surface were much stronger than those of $AgNO_3$, similar to Gluma desensitizers.

Effects of Silver Ions on Bovine Serum Albumin. *Circular Dichroism Response of Bovine Serum Albumin to Silver Ions.* The secondary structures of BSA were studied using CD spectroscopy. As shown in Figure 7A, all curves showed peaks at 208 and 220 nm representing the transition of the peptide bonds $\pi \rightarrow \pi^*$ and $n \rightarrow \pi^*$ in the α-helix of BSA. To analyze the detailed secondary structure changes, the contents of its components were measured (Table 1). The percentage of α-helices decreased, while the percentage of the β-sheet, β-turn, and random coils increased when BSA contacted both Ag^+ (24 h) and $AgNO_3$, indicating that Ag^+ led to the secondary structure alteration of BSA.

UV−Vis Spectroscopy. UV−vis spectroscopy was performed to study the conformational changes of BSA (Figure 7B). All spectra showed an absorption peak at 208 nm, indicating the peptide bond $\pi \rightarrow \pi^*$ transition of the

https://doi.org/10.1021/acsomega.1c02123
ACS Omega 2021, 6, 19596−19605

Table 1. Secondary Structure Fractions of Bovine Serum Albumin Altered by Ag^{+}[a]

solution	content (%)			
	α-helix	β-sheet	β-turn	random coil
BSA + SBF	61.0	7.7	13.8	17.5
BSA + Ag^{+} (24 h)	38.9	20.9	15.4	24.8
BSA + $AgNO_3$	41.3	19.2	15.2	24.3

[a]Abbreviations: bovine serum albumin (BSA), simulated body fluid (SBF), the supernatants of 4% Ag-MSNs@$n$$SiO_2$ dispersions mixed for 24 h [Ag^{+} (24 h)], and silver nitrate solution ($AgNO_3$) with the same concentration as that of Ag^{+} (24 h).

characteristic C═O-containing polypeptide backbone structure of BSA. With increasing Ag^{+} concentrations, the absorption peak decreased, suggesting that the skeleton structure originally buried in the hydrophobic layer was exposed to the polar environment, implying that the skeleton structure became more flexible.

Size Distribution Changes of Bovine Serum Albumin. To explore whether silver ions caused the aggregation of the BSA molecules, the size distributions of BSA were investigated (Figure 7C). In the control group, the average molecular hydrodynamic radius (RA) of BSA was 3.3 nm, which increased significantly to 5.3 nm in BSA + Ag^{+} (24 h) and to 6.2 nm in BSA + Ag^{+} (120 h); there was no significant difference between the latter two groups, suggesting that molecular expansion or oligomerization may have occurred between the BSA molecules (Figure 7D; $*P < 0.05$ vs BSA, $**P > 0.05$ vs BSA + Ag^{+} (120 h); $n = 3$).

DISCUSSION

In the present study, we synthesized a new material, Ag-MSNs@$n$$SiO_2$. With the characteristics of slow Ag^{+} release and nearly noncytotoxicity, Ag-MSNs@$n$$SiO_2$ effectively and immediately occluded dentinal tubules. Moreover, it induced structural changes of proteins in the dentine tubules, which may lead to protein condensation and maintain the blockage effects. Therefore, it may have good application prospects in the treatment of dentin hypersensitivity.

MSNs are nanoscale silica particles with hollow pores. Because of their high specific surface area and pore volume, MSNs could be used as carriers to encapsulate a series of drugs for subsequent slow release.[24] Besides, SiO_2 had high acid resistance stability to withstand the erosion of dietary acid.[6] This made it possible to encapsulate some substances and protect them from dietary acid erosion. In this experiment, we first synthesized MSNs with an average particle size of 128 nm, which is an advantage for filling dentinal tubules with a diameter of 2−3 microns (Figures 1A, 2A); the material was noncrystalline, consistent with the MSM-41 crystal type[25] (Figure 2B). To obtain pure and nontoxic MSNs, the cytotoxic intrapore surfactant, CTAC, was successfully extracted (Figure 2C).

Among the many loaded materials, silver nanoparticles were selected as the main component. However, silver ions have many disadvantages. Silver nanoparticles became another form of it we tried to introduce. Considering that the color of silver nanoparticles was different,[11] smaller size-silver nanoparticles have become the first choice for the color close to the teeth. In addition, the toxicity of small-sized silver nanoparticles is also affected by many factors.[26] In our experiment, the Ag-MSNs showed slow Ag^{+} release and a significant cytotoxicity (Figure 3A−D). The relative cell viability of Ag-MSNs was from 43 to 61% at the concentrations of 160 and 320 $\mu g\ mL^{-1}$, which were far below the basic requirements (70%) of biological materials.[27] Moreover, the direct contact of metal nanoparticles with cells may be one of the reasons for the high cytotoxicity of metal-loaded MSNs.[28] Therefore, a shell is needed to prevent direct contact between the Ag-MSNs and tissues, as well as to control the release of silver ions. SiO_2 is a component of MSNs. Coating with a silica shell is a promising method because of the excellent stability, biocompatibility, and nontoxicity of silica.[29] In our study, a layer of SiO_2 was coated onto the Ag-MSNs to obtain Ag-MSNs@$n$$SiO_2$ (Figures 1C, 2D−F). As shown in Figure 3A, the shell of SiO_2 significantly reduced the release of silver ions and the cytotoxicity of Ag-MSNs@$n$$SiO_2$ (Figure 3B−D). The relative cell viability of Ag-MSNs@$n$$SiO_2$ was all above 80%, significantly higher than Ag-MSN groups. Therefore, Ag-MSNs@$n$$SiO_2$ would be considered to have no a cytotoxic potential according to International Organization for Standardization,[27] which may mainly be due to the protection from the silica shells.

Under an electron microscope, we observed the immediate desensitization effects of Ag-MSNs@$n$$SiO_2$. The occluding effects were related to the concentration of Ag-MSNS@$n$$SiO_2$, and the effects of 4% were better than those of 2 and 6% (Figure 4). To evaluate the occluding effects of 4% Ag-MSNs@$n$$SiO_2$, deionized water (control group), 5.9 M $AgNO_3$ solution, and the Gluma desensitizer were selected for comparison. $AgNO_3$ was previously used as a dentin desensitizer, which exerted desensitizing effects through silver ions. Gluma desensitizers are commonly used desensitizers in clinic at present, whose active ingredients were 5% glutaraldehyde and 35% hydroxyethyl methacrylate.[30] Both $AgNO_3$ and Gluma desensitizers blocked dentin tubules through protein denaturation and aggregation. $AgNO_3$ blackened teeth due to the formation of silver oxide. In our experiment, the $AgNO_3$-treated dentine slices were blackened (Figure 5B), and their occluding effects were not as good as those of the 4% Ag-MSNs@$n$$SiO_2$ and the Gluma desensitizer (Figure 6A2−A4,B2−B4), which may be the reason why the traditional $AgNO_3$ had been eliminated but the Gluma desensitizer is widely used in clinic. The Gluma desensitizer formed a transverse septum-like substance in the dentin lumen (Figure 6B4) as previously reported.[31] The occluding effects of Gluma on the dentin surface were similar to that of 4% Ag-MSNs@$n$$SiO_2$ (Figure 6A3,A4,C), which blocked the dentinal tubules to a depth of up to 50 microns (Figure 6D). These results showed that Ag-MSNs@$n$$SiO_2$ rapidly and effectively occluded dentinal tubules as the Gluma desensitizer, but did not blacken dentin (Figure 5C). The immediate desensitization effect of Ag-MSNs@$n$$SiO_2$ was due to the size advantage of nanomaterials.

From Figure 3A, we knew that Ag-MSNs@$n$$SiO_2$ slowly released silver ions, and the concentration of silver ions increased over time. The concentration of silver ions depended on the concentration of the material itself and the thickness of the silica coating. It is well known that heavy metal ions caused aggregation and denaturation of protein molecules, which was microscopically manifested as a change in the multilevel structure of protein.[32] We speculated that silver ions slowly released from Ag-MSNs@$n$$SiO_2$ might cause protein aggregation in the dentin tubules and occluded dentinal tubules. Our results showed that silver ions released from Ag-MSNs@$n$$SiO_2$ significantly changed the secondary structure of BSA (Figure

https://doi.org/10.1021/acsomega.1c02123
ACS Omega 2021, 6, 19596−19605

7A, Table 1); the protein skeleton structure became looser (Figure 7B); and the average molecular hydrodynamic radius of BSA increased significantly (Figure 7C,D). The changes occurred slowly and continuously with the release of silver ions. Even if the nanomaterials on the surface of the dentin tubules were lost due to daily abrasion, the long-lasting effect of the silver ions released from the interior of the dentin tubules would continue, which is similar to the desensitization effects of glutaraldehyde, the active component of Gluma. Therefore, we believed that Ag-MSNs@nSiO$_2$ could block dentinal tubules stably and persistently.

CONCLUSIONS

Ag-MSNs@nSiO$_2$ was successfully synthesized by a series of methods, in which silver ions released slowly because of the encapsulation of MSNs and the protection of the silica shell. The relative cell viability of Ag-MSNs@nSiO$_2$ was all above 80%, significantly higher than Ag-MSNs groups, so was considered to have no cytotoxic potential according to International Organization for Standardization. Under an electron microscope, it rapidly and effectively sealed dentin tubules, but did not blacken dentin. Moreover, multilevel structures of BSA in dentin tubules were significantly changed by silver ions from Ag-MSNs@nSiO$_2$, which would enhance clogging effects in dentin tubules continuously. In conclusion, noncytotoxic Ag-MSNs@nSiO$_2$ was successfully synthesized, which occluded dentin tubules effectively and continuously. However, because this study is only a study in vitro, its effects need further clinical verification.

ASSOCIATED CONTENT

Supporting Information

The Supporting Information is available free of charge at https://pubs.acs.org/doi/10.1021/acsomega.1c02123.

Slow release of silver ions from Ag-MSNs and effects of the coating thickness on the release of silver ions (PDF)

AUTHOR INFORMATION

Corresponding Author

Yi Zhang − *Department of Stomatology, Chenggong Hospital Affiliated to Xiamen University, Xiamen 361000 Fujian province, China;* Present Address: Department of Stomatology, Chenggong Hospital Affiliated to Xiamen University, 92-96 Wenyuan Road, Siming District, Xiamen of Fujian province 361000, China; orcid.org/0000-0001-8268-8395; Phone: 0592-2136660; Email: xiamzy19@163.com

Authors

Yang Zhou − *Key Laboratory of Arrhythmias, Ministry of Education, Department of Medical Genetics, School of Medicine, Tongji University, Shanghai East Hospital, Shanghai 200120, China*

Meng Yang − *Department of Physiology, Medicine College, Jingchu University of Technology, Jingmen 448000 Hubei province, China*

Qingjie Jia − *Department of Biology, School of Life Sciences, Xiamen University, Xiamen 361005 Fujian, China*

Guojun Miao − *Key Laboratory of Arrhythmias, Ministry of Education, Department of Medical Genetics, School of Medicine, Tongji University, Shanghai East Hospital, Shanghai 200120, China*

Leilei Wan − *Department of Stomatology, Shanghai General Hospital, Shanghai 200080, China*

Complete contact information is available at: https://pubs.acs.org/10.1021/acsomega.1c02123

Notes

The authors declare no competing financial interest.

ACKNOWLEDGMENTS

This work was supported by Xiamen Municipal Bureau of Science and Technology in Fujian Province, China (no. 3502Z20174025) and Jingmen Science and Technology Bureau of Hubei Province, China (no.2018YFZD029).

REFERENCES

(1) Cummins, D. Dentin hypersensitivity: from diagnosis to a break through therapy for everyday sensitivity relief. *J. Clin. Dent.* **2009**, *20*, 1−9.

(2) Brännström, M. Dentin sensitivity and aspiration of odontoblasts. *J. Am. Dent. Assoc.* **1963**, *66*, 366−370.

(3) Miglani, S.; Aggarwal, V.; Ahuja, B. Dentin hypersensitivity: recent trends in management. *J. Conserv. Dent.* **2010**, *13*, 218−224.

(4) Canali, G. D.; Rached, R. N.; Mazur, R. F.; Souza, E. M. Effect of erosion/abrasion challenge on the dentin tubule occlusion using different desensitizing agents. *Braz. Dent. J.* **2017**, *28*, 216−224.

(5) Makvandi, P.; Josic, U.; Delfi, M.; Pinelli, F.; Jahed, V.; Kaya, E.; Ashrafizadeh, M.; Zarepour, A.; Rossi, F.; Ali, Z.; Agarwal, T.; Nazarzadeh Zare, E.; Ghomi, M.; Maiti, T. K.; Breschi, L.; Tay, F. R. Drug Delivery (Nano)Platforms for Oral and Dental Applications: Tissue Regeneration, Infection Control, and Cancer Management. *Adv. Sci.* **2021**, *8*, 2004014.

(6) Yu, J.; Yang, H.; Li, K.; Ren, H.; Lei, J.; Huang, C. Development of Epigallocatechin-3- gallate-Encapsulated Nanohydroxyapatite/Mesoporous Silica for Therapeutic Management of Dentin Surface. *ACS Appl Mater Interfaces* **2017**, *9*, 25796−25807.

(7) Tian, L.; Peng, C.; Shi, Y.; Guo, X.; Zhong, B.; Qi, J.; Wang, G.; Cai, Q.; Cui, F. Effect of mesoporous silica nanoparticles on dentinal tubule occlusion: an in vitro study using SEM and image analysis. *Dent. Mater. J.* **2014**, *33*, 125−132.

(8) Sharma, V. K.; Yngard, R. A.; Lin, Y. Silver nanoparticles: green synthesis and their antimicrobial activities. *Adv. Colloid Interface Sci.* **2009**, *145*, 83−96.

(9) Makvandi, P.; Gu, J. T.; Zare, E. N.; Ashtari, B.; Moeini, A.; Tay, F. R.; Niu, L.-n. Polymeric and inorganic nanoscopical antimicrobial fillers in dentistry. *Acta Biomater.* **2020**, *101*, 69−101.

(10) Krauser, J. T. Hypersensitive teeth, Part II: Treatment. *J. Prosthet. Dent* **1986**, *56*, 307−311.

(11) Agnihotri, S.; Mukherji, S.; Mukherji, S. Size-controlled silver nanoparticles synthesized over the range 5-100 nm using the same protocol and their antibacterial efficacy. *RSC Adv.* **2014**, *4*, 3974−3983.

(12) Martinez-Gutierrez, F.; Olive, P. L.; Banuelos, A.; Orrantia, E.; Nino, N.; Sanchez, E. M.; Ruiz, F.; Bach, H.; Av-Gay, Y. Synthesis, characterization, and evaluation of antimicrobial and cytotoxic effect of silver and titanium nanoparticles. *Nanomed. Nanotechnol. Biol. Med.* **2010**, *6*, 681−688.

(13) Jung, J.-H.; Kim, D.-H.; Yoo, K.-H.; Yoon, S.-Y.; Kim, Y.; Bae, M.-K.; Chung, J.; Ko, C.-C.; Kwon, Y. H.; Kim, Y.-I. Dentin sealing and antibacterial effects of silver-doped bioactive glass/mesoporous silica nanocomposite: an in vitro study. *Clin. Oral Invest.* **2019**, *23*, 253−266.

(14) Shen, D.; Yang, J.; Li, X.; Zhou, L.; Zhang, R.; Li, W.; Chen, L.; Wang, R.; Zhang, F.; Zhao, D. Biphase stratification approach to three-dimensional dendritic biodegradable mesoporous silica nanospheres. *Nano Lett.* **2014**, *14*, 923−932.

(15) Rostami, S.; Mehdinia, A.; Jabbari, A. Seed-mediated grown silver nanoparticles as a colorimetric sensor for detection of ascorbic acid. *Spectrochim. Acta, Part A* **2017**, *180*, 204−210.
(16) Stöber, W.; Fink, A. Controlled Growth of Monodisperse Silica Spheres in the Micron Size Range. *J. Colloid Interface Sci.* **1968**, *26*, 62−69.
(17) Zhu, Y.-f.; Shi, J.-l.; Li, Y.-s.; Chen, H.-r.; Shen, W.-h.; Dong, X.-p. Storage and release of ibuprofen drug molecules in hollow mesoporous silica spheres with modified pore surface. *Microporous Mesoporous Mater.* **2005**, *85*, 75−81.
(18) Kokubo, T.; Takadama, H. How useful is SBF in predicting in vivo bone bioactivity. *Biomaterials* **2006**, *27*, 2907−2915.
(19) Lang, O.; Kohidai, L.; Kohidai, Z.; Dobo-Nagy, C.; Csomo, K. B.; Lajko, M.; Mozes, M.; Keki, S.; Deak, G.; Tian, K. V.; Gresz, V. Cell physiological effects of glass ionomer cements on fibroblast cells. *Toxicol. in Vitro* **2019**, *61*, 104627.
(20) Ishihata, H.; Kanehira, M.; Finger, W. J.; Takahashi, H.; Tomita, M.; Sasaki, K. Effect of two desensitizing agents on dentin permeability in vitro. *J. Appl. Oral Sci.* **2017**, *25*, 34−41.
(21) De Munck, J.; Ermis, R. B.; Koshiro, K.; Inoue, S.; Ikeda, T.; Sano, H.; Van Landuyt, K. L.; Van Meerbeek, B. NaOCl degradation of a HEMA-free all-in-one adhesive bonded to enamel and dentin following two air- blowing techniques. *J. Dent. Res.* **2007**, *35*, 74−83.
(22) Lee, S. Y.; Kwon, H. K.; Kim, B. I. Effect of dentinal tubule occlusion by dentifrice containing nano-carbonate apatite. *J. Oral Rehabil.* **2008**, *35*, 847−853.
(23) Zhao, X.; Liu, R.; Teng, Y.; Liu, X. The interaction between Ag + and bovine serum albumin:A spectroscopic investigation. *Sci. Total Environ.* **2011**, *409*, 892−897.
(24) Li, Z.; Barnes, J. C.; Bosoy, A.; Stoddart, J. F.; Zink, J. I. Mesoporous silica nanoparticles in biomedical applications. *Chem. Soc. Rev.* **2012**, *41*, 2590−2605.
(25) Arrais, C. A. G.; Chan, D. C. N.; Giannini, M. Effects of desensitizing agents on dentinal tubule occlusion. *J. Appl. Oral Sci.* **2004**, *12*, 144−148.
(26) Makvandi, P.; Wang, C.-y.; Zare, E. N.; Borzacchiello, A.; Niu, L.-n.; Tay, F. R. Metal-Based Nanomaterials in Biomedical Applications: Antimicrobial Activity and Cytotoxicity Aspects. *Adv. Funct. Mater.* **2020**, *30*, 1910021.
(27) Rodrigues, M. C.; Rolim, W. R.; Viana, M. M.; Souza, T. R.; Gonçalves, F.; Tanaka, C. J.; Bueno-Silva, B.; Seabra, A. B. Biogenic synthesis and antimicrobial activity of silica- coated silver nanoparticles for esthetic dental applications. *J. Dent.* **2020**, *96*, 103327.
(28) Zhang, S.; Wen, L.; Yang, J.; Zeng, J.; Sun, Q.; Li, Z.; Zhao, D.; Dou, S. Facile Fabrication of Dendritic Mesoporous SiO_2@CdTe@SiO_2 Fluorescent Nanoparticles for Bioimaging. *Part. Part. Syst. Char.* **2016**, *33*, 261−270.
(29) Liu, Y.; Wang, P.; Wang, Y.; Zhu, Z.; Lao, F.; Liu, X.; Cong, W.; Chen, C.; Gao, Y.; Liu, Y. The Influence on Cell Cycle and Cell Division by Various Cadmium-Containing Quantum Dots. *Small* **2013l**, *9*, 2440−2451.
(30) Kara, H. B.; Cakan, U.; Yilmaz, B.; Inan Kurugol, P. Efficacy of Diode Laser and Gluma on Post-Preparation Sensitivity: A Randomized Split-Mouth Clinical Study. *J. Esthetic Restor. Dent.* **2016**, *28*, 405−411.
(31) Joshi, S.; Gowda, A. S.; Joshi, C. Comparative evaluation of NovaMin desensitizer and Gluma desensitizer on dentinal tubule occlusion: a scanning electron microscopic study. *J. Periodontal Implant Sci.* **2013**, *43*, 269−275.
(32) Tamás, M. J.; Sharma, S. K.; Ibstedt, S.; Jacobson, T.; Christen, P. Heavy Metals and Metalloids As a Cause for Protein Misfolding and Aggregation. *Biomolecules* **2014**, *4*, 252−267.

https://doi.org/10.1021/acsomega.1c02123
ACS Omega 2021, 6, 19596−19605